Int. J. Multiphase Flow Vol. 11, No. 6, pp. 797–812, 1985
Printed in Great Britain.

0301-9322/85 $3.00 + .00

ON THE MOTION OF LONG BUBBLES IN VERTICAL TUBES

KJELL H. BENDIKSEN
Institute for Energy Technology, Kjeller, Norway

(*Received* 10 *October* 1984; *in revised form* 30 *April* 1985)

Abstract—Potential flow theory has been applied to study the shape and speed of an infinitely long bubble rising through flowing liquid in a vertical tube. In particular, the combined effects of surface tension and externally forced liquid motion are examined. An analytical formula for the bubble rise velocity in stagnant liquid is proposed, and shown to be in good agreement with experimental data for all values of surface tension. Numerical solutions for the bubble velocity in upward flowing liquid are obtained for laminar and turbulent velocity profiles. Approximate expressions for the bubble velocity, where the effects of liquid motion and surface tension are incorporated through the Reynolds and inverse Eötwos numbers, are proposed and compared with experimental data. The predicted changes in bubble shape have, to a large extent, been confirmed through comparisons with photographic evidence for a wide range of parameters.

1. INTRODUCTION

The motion of single, large gas bubbles through stagnant liquid in vertical tubes under the influence of gravity, has been studied theoretically by several workers: Dumitrescu (1943), Davies & Taylor (1949) and Collins *et al.* (1978). Goldsmith & Mason (1962) included viscous forces, and Zukoski (1966) investigated the effect of surface tension experimentally.

The present study was initiated by the results of a more extensive series of experiments (Bendiksen 1984) on the motion of long bubbles through nonstationary liquid. It was shown that for all tube inclinations, θ, the bubble propagation rate is well represented by

$$v_B = C_0 v_L + v_0, \qquad [1]$$

where v_L is the average liquid velocity at infinity. For vertical or near vertical tubes with i.d. of about 2.5 cm, $C_0 \simeq 1.20$ for $\mathrm{Fr} \gtrsim 3.5$, quite independent of Re-number (3×10^4–10^5), and v_0 is close to the bubble rise velocity in stagnant liquid. The coefficient C_0 has been found to increase with decreasing Re-number, approaching 1.90 at $\mathrm{Re} \simeq 100$ (Nicklin *et al.* 1962). Thus, the bubble appears to propagate at a rate slightly less than the maximum liquid velocity at infinity plus v_0.

Collins *et al.* incorporated a dependency on the liquid velocity profile in their theoretical treatment, and obtained

$$v_B = v_m + v_0 \phi(v_m/\sqrt{gD}), \qquad [2]$$

where v_m is the liquid velocity at the tube axis at infinity, and the function ϕ (≥ 1) depends on the actual velocity profile. Their result, however, yields a value of C_0 slightly greater than the maximum to average liquid velocity ratio, e.g., 2.16 for laminar flow, but this apparent discrepancy with the experimental data will be shown to be due to their neglect of surface tension.

The present study is concerned with the motion of a single bubble through liquid in an infinitely long vertical pipe of circular cross-section. The liquid is assumed to be at rest or obeying a parabolic velocity profile at infinity, but turbulent velocity profiles, assumed parabolic near the axis, will also be investigated. The velocity field caused by the bubble motion is assumed to be axis-symmetric and irrotational.

A particular objective has been the combined effect of externally forced liquid motion and surface tension on bubble velocity and shape. The numerical solutions are found to be

well described by an extension of the Collins *et al.* formula [2], incorporating surface tension. The bubble velocity predictions also agree with the Nicklin slug formula [1], but the coefficients C_0 and v_0 depending on the Re- and inverse Eötwos-numbers. In short, the effect of more pointed liquid velocity profile is to increase the rise velocity, v_0, relative to that in stagnant liquid, and that of surface tension is to reduce it. The theoretical results have been compared with the data of Nicklin *et al.* (1962), Collins *et al.* (1978), Bendiksen (1984) for laminar and turbulent liquid flow and Zukoski (1966) for stationary liquid at infinity.

2. THEORY

2.1 *Basic equations*

A cylindrical coordinate system (r, ϕ, z) following the bubble is applied, as shown in figure 1. The neglect of viscosity is justified by observing that the growth of the two boundary layers created, at the wall and at the bubble surface, will be slow, and also prevented by the acceleration of the liquid around the bubble nose, provided the Re-number, $\mathrm{Re}_B = \rho_L v_B D/\mu$ is high. This treatment will therefore be limited to the inertia dominated regime, which covers most practical cases, and where $\mathrm{Re}_B \gtrsim 100$. Because these boundary layers are thin, the pressure distribution is well represented by irrotational flow when the bubble rises through stagnant liquid (Dumitrescu 1943) and by a rotational flow with a prescribed vorticity distribution far upstream when the bubble rises through flowing liquid. The effect of viscosity is then to generate the actual velocity profile far upstream, whereas the liquid motion due to the bubble is assumed to be inviscid and irrotational (Batchelor 1980; Collins *et al.* 1978). Assuming rotational symmetry around the z-axis, and steady bubble motion, the vorticity, ω_ϕ, may be expressed as

$$\omega_\phi = -\frac{1}{r}\left(\frac{\partial^2\psi}{\partial z^2} + \frac{\partial^2\psi}{\partial r^2} - \frac{1}{r}\frac{\partial\psi}{\partial r}\right), \qquad [3]$$

where ψ is the stream function.

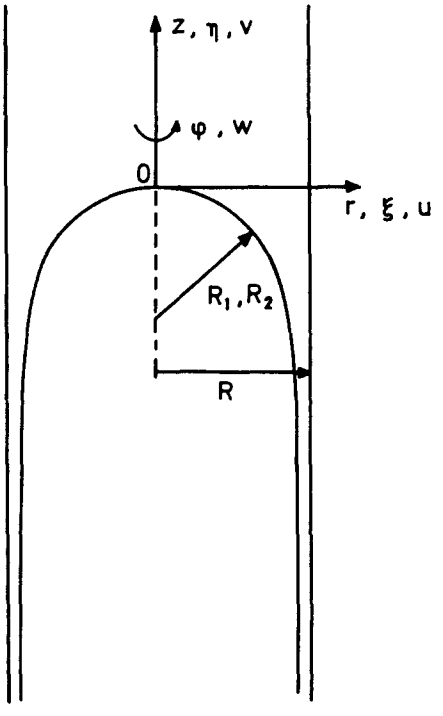

Figure 1. The applied coordinate system.

For purely inertial flow under the influence of gravity, only, dimensional analysis yields $v_0 = v_0^* \sqrt{gR}$, and to obtain nondimensional equations we use

$$\eta = z/R,\ \xi = r/R,\ u^* = u/\sqrt{gR},\ v^* = v/\sqrt{gR},\ \psi^* = \psi/\sqrt{gR^5},$$

where the star indicates a dimensionless quantity, which will be subsequently dropped, whenever there is no possibility of confusion.

The dimensionless bubble velocity may, without loss of generality, be expressed as

$$v_B = v_m + C(\Sigma, v_m) + v_0, \qquad [4]$$

where $v_0 = v_0(\Sigma)$ is the rise velocity in stagnant liquid, and $C(\Sigma, v_m)$ is the deviation from v_0 caused by an upward moving liquid at infinity with velocity v_m at the tube axis.

Assuming a parabolic (or zero) liquid velocity profile at infinity, the boundary condition at $\eta = \infty$, in a frame of reference following the bubble nose, becomes

$$v_L^\infty(\xi) = v_m(1 - \xi^2) - v_m - C(\Sigma, v_m) - v_0 \qquad [5]$$

or

$$\psi^\infty(\xi) = -\tfrac{1}{4} v_m \xi^4 - \tfrac{1}{2} v_{0m} \xi^2, \qquad [6]$$

where

$$v_{0m} = v_0 + C(\Sigma, v_m) \qquad [7]$$

and the inverse Eötwos number, $\Sigma = \sigma/(\rho_L g R^2)$. In the applied reference system the motion is steady, and with $\omega_z = \omega_r = 0$, ω_ϕ may be obtained from [3] in nondimensional notation as

$$\omega_\phi = 2 v_m \xi. \qquad [8]$$

Then [3] may be written on dimensionless form as

$$\frac{\partial^2 \psi}{\partial \xi^2} + \frac{\partial^2 \psi}{\partial \eta^2} - \frac{1}{\xi} \frac{\partial \psi}{\partial \xi} = -2 v_m \xi^2. \qquad [9]$$

A solution of [9] is most easily obtained by decomposing the stream-function into its up-stream value and local deviation from this (see, for instance, Batchelor 1980, pp. 544):

$$\psi(\xi, \eta) = -\frac{1}{2} v_{0m} \xi^2 - \frac{v_m}{4} \xi^4 + \xi F(\xi, \eta). \qquad [10]$$

Equation [9] then yields an equation for F

$$\frac{\partial^2 F}{\partial \eta^2} + \frac{\partial^2 F}{\partial \xi^2} + \frac{1}{\xi} \frac{\partial F}{\partial \xi} - \frac{F}{\xi^2} = 0. \qquad [11]$$

A well-known solution of [11] satisfying the boundary condition $u = 0$ at the tube surface and being bounded everywhere, provided $\eta > -\infty$, is obtained by the method of separation of variables, and is given by

$$F(\xi, \eta) = \sum_i k_i J_1(\beta_i \xi)\, e^{-\beta_i \eta}, \qquad [12]$$

where β_i are the ith zeros of the Bessel function of the first kind and order. The complete stream-function is then

$$\psi(\xi, \eta) = -\frac{v_{0m}}{2}\xi^2 - \frac{v_m}{4}\xi^4 + \xi \cdot \sum_i k_i J_1(\beta_i \xi)\, e^{-\beta_i \eta} \qquad [13]$$

and the velocities are given by

$$\begin{aligned} u &= +\sum_i k_i \beta_i J_1(\beta_i \xi)\, e^{-\beta_i \eta}, \\ v &= -v_{0m} - v_m \xi^2 + \sum_i k_i \beta_i J_0(\beta_i \xi)\, e^{-\beta_i \eta}. \end{aligned} \qquad [14]$$

2.2 *Boundary conditions*

The conditions already satisfied in [13] and [14] are those at $\eta = +\infty$ ([5] and [6]) and at the tube surface, $\xi = 1$, where $u(1, \eta) = 0$ for all η.

The boundary condition at the bubble surface is more complicated, due to the bubble shape being unknown. If the pressure in the bubble is assumed to be constant p_G^0 ($\rho_G \ll \rho_L$), the pressure in the liquid at the interface may be approximated as

$$p_L(z) = p_G(z) - \sigma\left(\frac{1}{R_1(z)} + \frac{1}{R_2(z)}\right), \qquad [15]$$

where R_1, R_2 are the effective local radii of curvature in and perpendicular to the rz-plane. In the applied coordinate system, $z = r = 0$ is a stagnation point, and assuming that the bubble surface is also a stream-line, Bernoullis equation yields

$$\frac{p_L(z)}{\rho_L} + \frac{1}{2}(u^2 + v^2) - g|z| = \frac{p_L^0}{\rho_L}. \qquad [16]$$

Substituting the liquid pressure, p_L, from [15] we get

$$u^2 + v^2 = 2g|z| - \frac{2\sigma}{\rho_L}\left[\left(\frac{1}{R_1(0)} + \frac{1}{R_2(0)}\right) - \left(\frac{1}{R_1(z)} + \frac{1}{R_2(z)}\right)\right] \qquad [17]$$

or on nondimensional form

$$u^2 + v^2 = 2|\eta| - 2 \cdot \Sigma \cdot \left[\left(\frac{1}{R_1(0)} + \frac{1}{R_2(0)}\right) - \left(\frac{1}{R_1(\eta)} + \frac{1}{R_2(\eta)}\right)\right].$$

The radii of curvature are rather complicated functions, which will be derived from [13]. First, observe that [14] at the stagnation point ($\xi = \eta = 0$) yields

$$v_{0m} = \Sigma k_i \beta_i, \qquad [18]$$

which determines v_{0m} as a function of the constants k_i, β_i. An equation for the bubble shape is then obtained from [13] and [18]:

$$\frac{1}{2}\xi \sum_i k_i \beta_i + \frac{v_m}{4}\xi^3 - \sum_i k_i J_1(\beta_i \xi)\, e^{-\beta_i \eta} = 0 \qquad [19]$$

on the bubble surface ($\psi = 0$).

The other boundary condition [17], using [14] and [18], yields

$$\left(\sum_i k_i\beta_i J_1(\beta_i\xi)\,e^{-\beta_i\eta}\right)^2 + \left(\sum_i k_i\beta_i + v_m\xi^2 - \sum_i k_i\beta_i J_0(\beta_i\xi)\,e^{-\beta_i\eta}\right)^2 = 2|\eta| - 2\cdot\Sigma\left[\frac{1}{R_0} - \frac{1}{R(\eta)}\right], \quad [20]$$

where $1/R(\eta) = 1/R_1(\eta) + 1/R_2(\eta)$.

Except for the surface tension terms Dumitrescu (1943) obtained an equivalent set of equations for the special case of no motion at $\eta = +\infty$ ($v_m = 0$). In order to solve [18]–[20], however, keeping three terms in the series expansion, he had to impose an additional boundary condition in $\eta = -\infty$. This replaces one of the equations, and reduces the complexity of the problem considerably, but it does lead to an overdetermined solution. Furthermore, he assumed a spherical bubble shape at origo, and this actually leads to a double solution.

In the following, [18]–[20] are therefore solved directly, making no apriori assumptions on bubble shape. Provided an explicit equation for the bubble surface on the form $\eta = \eta(\xi)$ may be found, the principal radii of curvature are easily shown to be given by

$$\frac{1}{R_1(\eta)} + \frac{1}{R_2(\eta)} = \left\{-\frac{\partial^2\eta}{\partial\xi^2}\left[1 + \left(\frac{\partial\eta}{\partial\xi}\right)^2\right]^{-1} + \frac{1}{\xi}\left|\frac{\partial\eta}{\partial\xi}\right|\right\}\left[1 + \left(\frac{\partial\eta}{\partial\xi}\right)^2\right]^{-1/2} \quad [21]$$

where the second term has to be replaced by its limit as $\xi \to 0$.

2.3 *Power series solution*

The problem is now to determine the coefficients k_i so that ξ, η satisfies [19] and [20] simultaneously.

Retaining N terms in [19] and [20], there are three obvious angles of attack in solving the resulting $2N$ equations. The first is a purely numerical one; choosing different ξ_i, $i = 1, N$ we get $2N$ unknowns ($k_1, k_2, \ldots, k_N, \eta_1, \eta_2, \ldots, \eta_N$). Another approach is to utilize the orthogonality properties of the Bessel functions to get an explicit expression $\eta = \eta(\xi)$. This method was investigated, and will work, provided the velocity profile in the film at $\eta = -\infty$ may be assumed known. This, however, seems a rather severe assumption, of the same nature as that of Dumitrescu (1943). Therefore, the expansion of the Bessel and exponential functions in power series, also applied by him, was finally chosen.

A power series expansion of the Bessel and exponential functions in [19] to $O(\xi^6)$ is shown in the Appendix to yield an explicit equation for the bubble surface [A6] on the form $\eta = \eta(\xi)$. Similarly, the boundary condition [20] reduced to [A9]. Inserting the explicit expression for η into the boundary condition [A9], applying the radii of curvature from [A11], yields an equation in ξ^{2i}, $i = 1, 2, 3$, only [A13].

The applied method of solution consists of collecting terms of order ξ^2, ξ^4, ξ^6 and determine the coefficients k_i, $i = 1, 2, 3$ from the three resulting equations. To avoid the last, and most complicated equation, Dumitrescu (1943) introduced the boundary condition in $\eta = -\infty$, as remarked in the past section.

After some algebra the equations become, from [A13]

$$B_2^3 = \tfrac{1}{8}B_{3v} + 8\cdot\Sigma\cdot B_2\cdot(b_2 - b_1^3), \quad [22a]$$

$$5B_{3v}^2 - 4B_2B_4 - 2\frac{B_2^2}{B_3}B_5 - 2B_{3v}\cdot v_m - \frac{1}{2}a_2B_3^{-1} - \Sigma\left[72(b_3 - 4b_1^2b_2 + 2b_1^5) + 16\frac{B_5}{B_3}(b_2 - b_1^3)\right] = 0, \quad [22b]$$

$$\left[\frac{B_3}{B_2}B_{3v}^2 + 2B_{3v}(B_3 + v_m) + 2B_2B_5\right]B_4 + B_3B_4^2$$
$$+ \left\{-\left[\frac{v_m}{2}\left(\frac{B_3}{B_2}\right)^2 + \frac{3}{2}B_5\right]B_{3v} - 3B_3B_5\right\}B_{3v} + \frac{2}{3}B_2B_3B_6$$
$$+ 2B_2(1 - v_m)a_2 - \frac{1}{2}a_3 - \Sigma\,[64B_3(b_4 + 30b_1^4b_2 - 10b_1 - 12b_1b_2^2 - 9b_1^2b_3) \qquad [22c]$$
$$- 36B_5(b_3 - 4b_1^2b_2 + 2b_1^5)] = 0.$$

These three equations yield the unknown coefficients $B_{2\text{-}4}$, from which the k_i's are obtained by solving the linear set [A2]:

$$\sum_i^N k_i\left(\frac{\beta_i}{2}\right)^m = B_m; \quad m = 2, \ldots, N + 1. \qquad [23]$$

Actually, the set [22] has to be solved iteratively, as the coefficients B_m, $m \geq 5$ also are given by [23]. This is *not* a closure problem, but rather a consequence of introducing the short-hand notation B_m; the real unknowns are the coefficients k_i, $i = 1, 3$, for which we do have three equations. Incidentally, there is a closure problem associated with the surface tension terms, as stated in the Appendix. If the interface condition [20] is sought to $O(\xi^6)$, because of the presence of first- and second-order derivatives of the bubble surface equation [19] it has to be of $O(\xi^8)$ for the sixth-order term in [20] to be accurate.

2.4 *Numerical method*

Equations [22], [23] and [18] have been solved numerically for different values of surface tension parameter, Σ, and liquid velocity in $\eta = \infty$, v_m. Since the coefficients $b_i = b_i(B_j)$, $j = 2, 8$, an iterative procedure is required for the solution of $B_{2\text{-}4}$ from [22] with $B_{5\text{-}8}$ from [23]. The outer loop yields B_3 from [22b]. For a given B_3 the inner iteration then consists of solving [22a, c] for B_2 and B_4, simultaneously. For $\Sigma \ll 1$ the B_2-calculation may be decoupled from that of B_4, which is a very significant simplification. It is also numerically advantageous to start the B_2-calculation with $B_2 = \frac{1}{2}B_{3v}^{1/3} + \Delta(\rho)$, where $\Delta \ll B_3$. If the resulting changes in $B_{5\text{-}8}$ are greater than, say 1%, the outer iteration is repeated with the same B_3-values, but with $B_n = (B_n^{\text{old}} + B_n^{\text{new}})/2$, $n = 5, \ldots 8$. For $\Sigma \ll 1$ this proved unnecessary, if the initial values were properly selected, for example from the analytical expressions [30] or [31]. For $\Sigma \gtrsim 0.10$ with $N = 3$ the method fails, as might be expected, due to the large deformation of the bubble requiring increasingly higher order terms in [19], [20]. However, as will be shown, in this region the analytical formulas still yield surprisingly good results. With our choice of coordinate system, $v_0 \geq 0$, and $R_0 \geq 0$ require B_2, $B_3 \geq 0$. With this assumption we always found a unique solution, if it existed at all.

2.5 *Analytical expression for the bubble velocity*

Because of the surface tension terms, [22] had to be solved numerically. Based on the physical features of the problem, however, a very simple analytical expression for the bubble velocity may be obtained as follows. The basic idea is to reformulate [22a, b] in terms of the mean radius of curvature at the nose (ρ), and replace [22c] by a known relation

$$\rho = \rho(\Sigma). \qquad [24]$$

Then, from [A11] we get, with $\rho = R_i(0)$, $i = 1, 2$,

$$\rho = \frac{1}{2b_1} = \frac{2B_3}{a_1} = \frac{2B_2}{B_{3v}}. \qquad [25]$$

Rearranging [22a] yields:

$$2B_2 = B_{3v}^{1/3}[1 + 64 \cdot \Sigma \frac{B_2}{B_{3v}}(b_2 - b_1^3)]^{1/3}. \quad [26]$$

Equation [25] then yields

$$B_{3v} = \left(\frac{1}{\rho}\right)^{3/2}[1 + \Sigma \cdot f(\rho)]^{1/2} \quad [27]$$

and

$$B_2 = \tfrac{1}{2}\{(1/\rho)[1 + \Sigma \cdot f(\rho)]\}^{1/2},$$

where $f(\rho)$ depends on N:

$$f(\rho) = 64(B_2/B_{3v})(b_2 - b_1^3). \quad [28]$$

For $N = 1$, using [23] the computation is straightforward and yields

$$f_1(\rho) = \tfrac{4}{3} \cdot \rho^{-2}$$

and for $N = 2$ it becomes

$$f_2(\rho) = 4\left\{-5\rho^{-2} + \frac{1}{3(\beta_2 - \beta_1)}\left[\left(\beta_2 - \frac{4}{\rho}\right)\left(\frac{\beta_1}{2}\right)^2\left(6 - \frac{\beta_1}{2}\rho\right) + \left(\frac{4}{\rho} - \beta_1\right)\left(\frac{\beta_2}{2}\right)^2\left(6 - \frac{\beta_2}{2}\rho\right)\right]\right\}. \quad [29]$$

For $N \leq 2$ the closed expressions for the bubble velocity then follow from [23] and [18]. If $N \geq 3$ additional equations [22b, c, . . .] for the coefficients B_4, B_5, . . . are required, and these soon become prohibitively complicated. With $N = 1$, however, the calculation again is straightforward and yields

$$v_0(\Sigma) = \beta_1^{-1/2}(1 + \tfrac{4}{3}\Sigma\rho^{-2})^{1/2}, \quad [30]$$

where from [25]

$$\rho = 4/\beta_1 = 1.0439.$$

For $N = 2$ [23] with B_m from [27] reduces, after some more algebra, to a rather simple expression

$$v_0(\Sigma) = 2\frac{\beta_1 + \beta_2}{\beta_1\beta_2}\rho^{-1/2}\left(1 - \frac{4}{\beta_1 + \beta_2}\rho^{-1}\right) \cdot [1 + \Sigma \cdot f_2(\rho)]^{1/2}, \quad [31]$$

where $\beta_1 = 3.8317$ and $\beta_2 = 7.0156$.

It follows from [30] that keeping the first term, only, although giving a rather accurate bubble velocity for $\Sigma = 0$, leads to an incorrect dependence on surface tension. The radii of curvature [24] may be obtained by the method of the past section, which yields relation [44], or from experiments. The relation [29] for f_2 is well approximated for $\Sigma \lesssim 0.7$ by

$$f_2 = 5(1 - 1.7\Sigma),$$

when ρ is given by [44]. This simplifies [31] considerably:

$$v_0(\Sigma) = 0.486\sqrt{1 + 5(1 - 1.72\Sigma)\Sigma} \cdot \frac{1 - 0.96\, e^{-0.066/\Sigma}}{1 - 0.52\, e^{-0.066/\Sigma}} \qquad [32]$$

A comparison with experiment to be presented in the next chapter (figure 2) shows very good agreement with [31] and [32] for all values of Σ.

2.6. *Turbulent profiles*

Consider the following modification of [13]:

$$\psi(\xi, \eta) = -\tfrac{1}{2}v_{0m}\xi^2 - \tfrac{1}{4}\gamma v_m\xi^4 + \xi \sum_i k_i J_1(\beta_i\xi)\, e^{-\beta_i\eta}, \qquad [33]$$

where γ represents a deviation from the parabolic velocity profile at $\eta = \infty$. Clearly [33] does not satisfy [3] at all points in the flow, except when it is parabolic at infinity ($\gamma = 1$), but it does describe a flow which is irrotational on the tube axis and close to the stagnation point, as any solution of [3] must be. As remarked by Collins *et al.* (1978), [33] will give an erroneous convection of vorticity around the bubble nose. Applying a particular turbulent velocity profile, however, being parabolic near the axis, is expected to reduce the effect of this deficiency.

The liquid velocity profile at $\eta = \infty$ is then replaced by the Pai approximation to the universal velocity profile:

$$v_L(\xi) = v_m[1 - \gamma\xi^2 - (1 - \gamma)\xi^{2n}], \qquad [34]$$

where n is a large, Re-dependent number. Applying the velocity defect law

$$[v_m - v_L(\xi)]/u_* = \phi(\xi) \qquad [35]$$

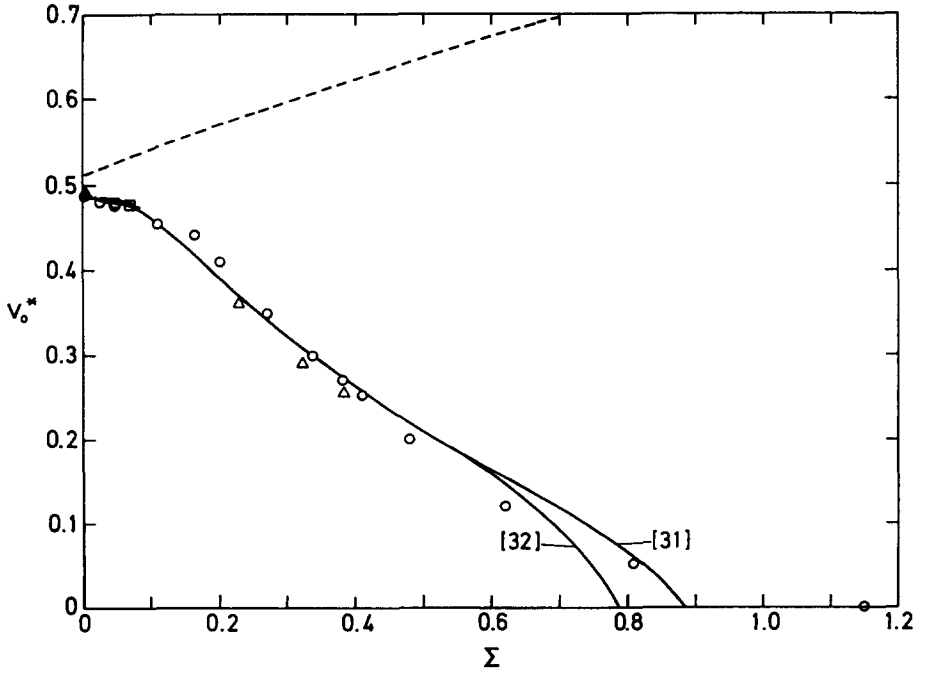

Figure 2. The influence of surface tension (Σ) on bubble velocity in stagnant liquid (Theoretical: – · – 3 terms, — 2 terms [31], – – – 1 term [30]. Experimental: Zukoski (1966): O Air/Water, Δ Alcohol/Water. Bendiksen (1984): □ Air/Water).

with the Reichardt's approximation to ϕ

$$\phi(\xi) = 2.5 \ln [(1 + 2\xi^2)/(1 - \xi^2)]$$

yields an approximation on the same form as the Pai profile [34] for $\xi \ll 1$:

$$v_L(\xi) = v_m[1 - \gamma\xi^2] \qquad [36]$$

and $\gamma = 7.5u_*$. The friction velocity, u_*, is defined by

$$u_* = \sqrt{\tau_w/\rho_L} = \bar{v}_L\sqrt{1/2 f}, \qquad [37]$$

where τ_w is the shear stress at the wall. Specifying the friction factor, f, e.g., that of Collins *et al.* (1978),

$$f^{-1/2} = 3.5 \log \mathrm{Re} - 2.6,$$

where $\mathrm{Re} = \rho_L v_L D/\mu_L$, yields the friction velocity and finally γ:

$$\gamma = 7.5[4.12 + 4.95(\log \mathrm{Re} - 0.743)]^{-1}. \qquad [38]$$

The velocity profile [36] with γ from [38] is then applied in [33]. Since a frame of reference following the bubble nose has been used, it suffices to replace [5] and [6] by

$$v_L^{\infty}(\xi) = v_m(1 - \gamma\xi^2) - v_B = -v_{0m} - \gamma v_m\xi^2 \qquad [39]$$

and

$$\psi^{\infty}(\xi) = -1/2 v_{0m}\xi^2 - 1/4 \gamma v_m \xi^4 \qquad [40]$$

or to replace v_m by γv_m in the equations to be solved [18]–[20]. The results will be presented in the next section.

3. RESULTS

3.1. *Bubble motion*

Stagnant liquid. The influence of surface tension on bubble velocity is shown in figure 2 for $v_m = 0$. The theoretical values are presented for $N = 1 - 3$, and the measurements are from Zukoski (1966) and Bendiksen (1984). For $\Sigma = 0$ $v_0^* = 0.511$, 0.487 and 0.495, respectively, and the latter compares very well with that of Dumitrescu (1943) of 0.496 based on asymptotic matching. Keeping the first term of the series [19] and [20], only, yields a somewhat too high value of 0.511, in contrast to that reported by Davies and Taylor (1949) of 0.464. The latter, however, was obtained for $\xi = 1/2$, and this, obviously, is inconsistent with the assumption $\xi \ll 1$, permitting the higher order terms to be neglected. For $\xi \to 0$, the result of Davies and Taylor does, in fact, approach 0.511.

The analytical expressions [31] and [32] are applied for $\Sigma > 0.10$ with radii of curvatures at the nose from the theoretical calculation. For $\Sigma \lesssim 0.4$ the predictions agree to within $1 \to 5\%$ for $N \geq 2$, whereas keeping the first term, only, is clearly insufficient to reproduce the observed dependence on surface tension. Although higher order terms in [19] and [20] are needed for $\Sigma \gtrsim 0.1$, the analytical expression [32] with ρ extrapolated from figure 6, [44], is surprisingly accurate.

Laminar profiles. A convenient way of representing the effect of a liquid velocity profile at infinity is through the distribution slip parameter, C_0, defined by [1].

It is seen from figure 3 that for $\Sigma = 0$, $C_0 \simeq 2.29$ and the bubble actually moves faster than the center liquid at infinity, plus v_0. This is in accordance with earlier results for purely viscous flow with $v_0 = 0$, where the acknowledged value is $C_0 \simeq 2.27$ for $\Sigma = 0$ (Taylor 1962). This rather surprising result, also obtained by Collins *et al.* (1978) may be qualitatively understood from the Bernoulli equation [16]. A parabolic instead of a flat velocity profile at infinity increases the liquid flow in the $-\eta$ direction close to the bubble surface, in a frame of reference attached to the bubble nose. This implies an increase in the rise velocity, and would cause a bubble drift velocity ($v_B > v_m$) even in the limit of zero gravity. This added drift velocity is proportional to the liquid velocity, with, as will be shown, a coefficient of proportionality dependent on the velocity profile, 0.29 for laminar flow. This is the cause of the calculated increase in C_0 (figure 3).

The effect of surface tension is to reduce the bubble velocity, and the combined effect is well described by an extension of the Collins *et al.* (1978) formula [2], in dimensional notation:

$$v_B = v_m + v_0\phi(v_m, \Sigma). \qquad [41]$$

For $\Sigma < 0.1$ the following extension of the Nicklin slug formula is recommended (see figure 3):

$$v_B = 2.29[1 - 5\Sigma(1 - e^{-0.05/\Sigma})]v_L + v_0^*(\Sigma)\sqrt{gR}, \qquad [42]$$

where $v_0^*(\Sigma)$ is given by [32].

The predicted value for C_0 of 1.94 for $\Sigma = 0.046$ is in reasonable agreement with the experimentally observed ones of from 1.80 to 1.95 (Nicklin *et al.* 1962).

Turbulent profiles. The numerical predictions for the bubble velocity are presented in figure 4 through the distribution slip parameter, C_0, using the drift velocities, $v_0^*(\Sigma)$, for stagnant liquid from figure 2.

The numerical results are, as for laminar flow, well described by the Nicklin slug formula [1], but with coefficients C_0, v_0 dependent on Re-number and Σ. For $\Sigma \lesssim 0.1$ the following extension of the Collins *et al.* (1978) formula for C_0, reproduces the numerical

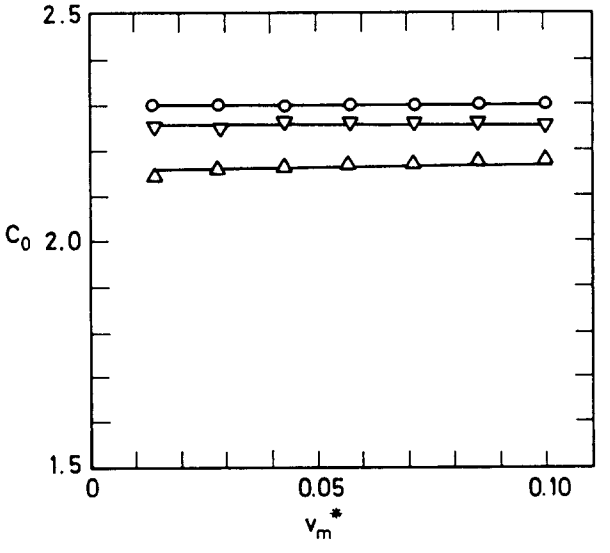

Figure 3. The dependence of C_0 [1] on laminar liquid velocity at infinity (v_m^*) with surface tension as parameter ($O\Sigma = 0$, $\nabla\Sigma = 0.0026$, $\Delta\Sigma = 0.013$, — [42]).

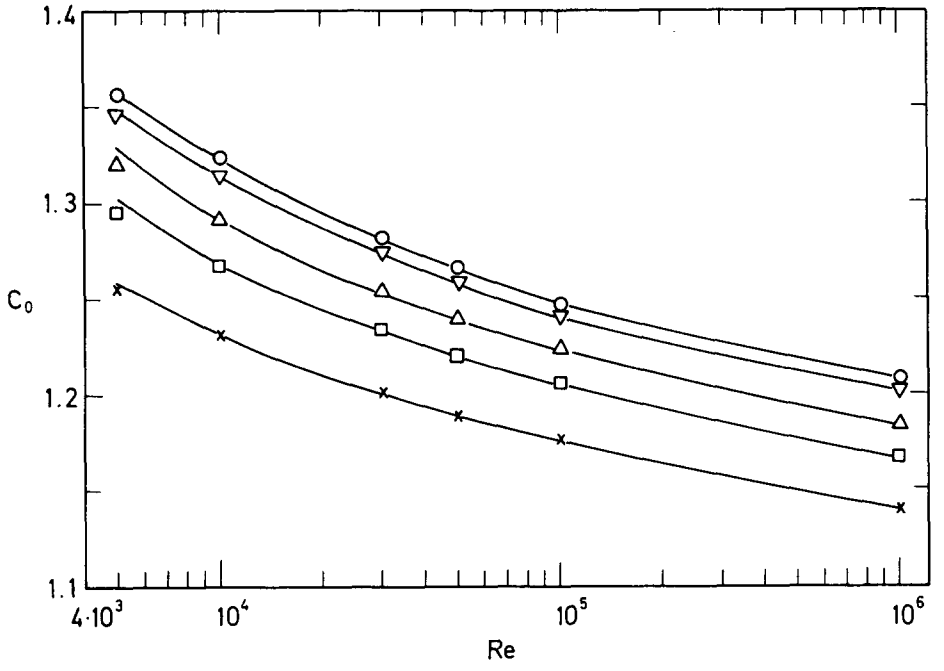

Figure 4. The dependence of C_0 [1] on Re-number for turbulent liquid flow at infinity with surface tension as parameter (○, ▽, △, □, × Σ = 0, 0.0026, 0.013, 0.026, 0.065, — [43]).

results very well (figure 4):

$$C_0 = \frac{\log \mathrm{Re} + 0.309}{\log \mathrm{Re} - 0.743}\left[1 - \tfrac{1}{2}\Sigma(3 - \log \mathrm{Re}\, e^{-0.1/\Sigma})\right] \qquad [43]$$

and $v_0(\Sigma) = v_0^*(\Sigma)\sqrt{gR}$, with v_0^* from [32].

The increase in bubble rise velocity due to the imposed liquid velocity profile decreases with increased Re-number, due to the flattening of the profile.

Relation [43] has been compared with the air–water experimental data of Bendiksen (1984) in figure 5, and the agreement is good. The maximum to average liquid velocity ratio

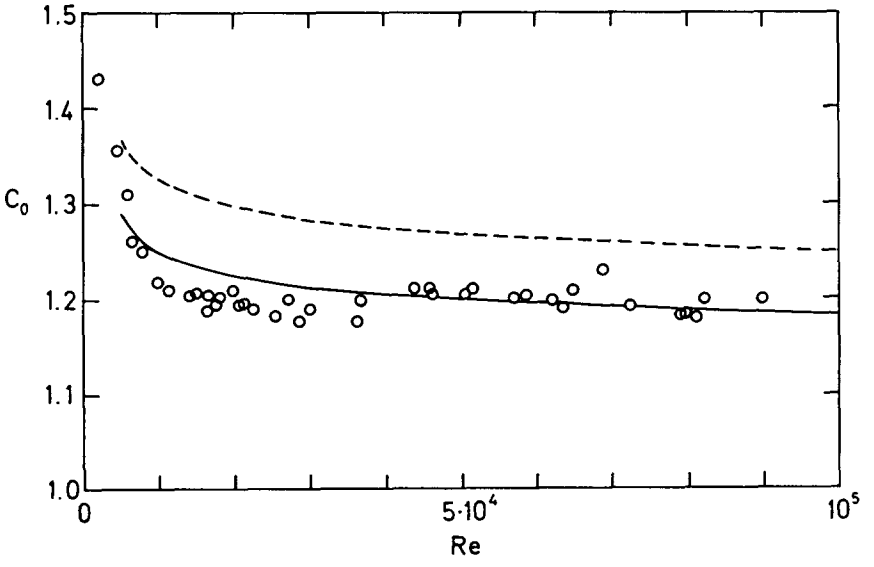

Figure 5. A comparison of predicted and measured distribution slip parameters, C_0 (○Σ = 0.042 Data of Bendiksen (1984), — [43] with Σ = 0.042, ---- [43] with Σ = 0).

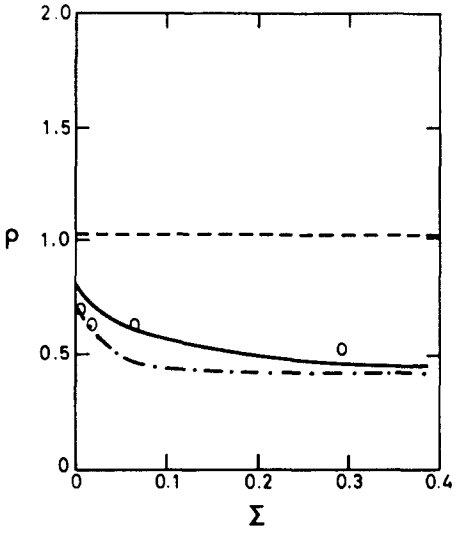

Figure 6. Predicted radius of curvature at origo, ρ, vs surface tension for $v_m = 0$ [– · – $N = 3$, — $N = 2$, – – – $N = 1$, O Data of Dumitrescu (1943)].

decreases from about 1.23 to 1.20 in the actual Re-number interval (3×10^4–10^5), and the measurements and predictions [43] are both below this, due to the effect of surface tension. Decreasing Σ, for instance by increasing the tube i.d. (from the 2.42 cm applied in the experiments), would shift C_0 towards the upper curve in figure 5.

3.2. *Bubble shape*

The principal radius of curvature at origo with N terms in [19, 20], ρ, is shown in figure 6 for $N = 1, \ldots, 3$. It is believed that the predicted fall in ρ with Σ for $N = 3$ is slightly too large. The extrapolated values to be applied in the analytical velocity formula [31] are very well represented, for $\Sigma \leq 1$, by

$$\rho(\Sigma) = \rho_0(1 - c_1 e^{-c_2/\Sigma}), \qquad [44]$$

where $\rho_0 = 0.795$, $c_1 = 0.5173$, and $c_2 = 0.0661$. The predicted decrease in ρ with increasing Σ

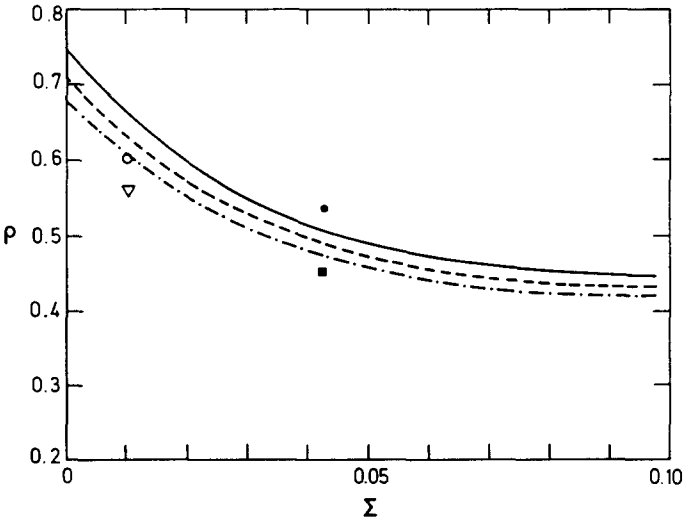

Figure 7. Predicted and measured effects of liquid motion at infinity and surface tension on bubble shape at origo (ρ) (Predictions: — $v_m^* = 0$, – – – $v_m^* = 0.05$, – · – $v_m^* = 0.10$. Data of Collins *et al.* (1978): O$v_m^* \approx 0.05$, ∇$v_m^* \approx 0.10$, Data of Bendiksen (1984): ●$v_m^* = 0.07$, ■$v_m^* = 0.9$).

has been confirmed by the experiments of Dumitrescu (1943) (figure 6). For large Σ increasingly higher order terms are required, as well as the incorporation of the exact bubble surface equation [A3] in the calculation of R_1, R_2, to represent the break-point near the wall.

The substantial increase in complexity, however, makes this an extremely doubtful procedure, particularly in view of the methodical limitations, and the only marginal potential improvements with respect to the velocity formula [31].

A last important effect is the predicted increase in curvature near origo caused by liquid motion at infinity (figure 7). This has been qualitatively confirmed by photographic evidence from a series of experiments (Bendiksen 1984; Collins *et al.* 1978). Actually this effect was observed for other inclinations as well, even in horizontal tubes.

Acknowledgements—I am grateful to Dr. A. Bertelsen for his very constructive advice.

REFERENCES

BATCHELOR, G. K. 1980 An introduction to fluid dynamics. Cambridge University Press, England.

BENDIKSEN, K. H. 1984 An experimental investigation of the motion of long bubbles in inclined tubes. *Int. J. Multiphase Flow,* **10,** 467–483.

COLLINS, R., DE MORAES, F. F., DAVIDSON, J. F., & HARRISON, D. 1978 The motion of a large gas bubble rising through liquid flowing in a tube. *J. Fluid. Mech.* **89,** 497–514.

DAVIES, R. M. & TAYLOR, G. I. 1949 The mechanics of large bubbles rising through extended liquids and through liquids in tubes. *Proc. Roy. Soc. London* **200A,** 375–390.

DUMITRESCU, D. T. 1943 Strömung an einer Luftblase im senkrechten Rohr. *Z. angew. Math. Mech.* **23,** 139–149.

GOLDSMITH, H. L. & MASON, S. G. 1962 The motion of single large bubbles in closed vertical tubes. *J. Fluid Mech.* **14,** 42–58.

NICKLIN, D. J., WILKES, J. O. & DAVIDSON, J. F. 1962 Two-phase flow in vertical tubes. *Trans. Inst. Chem. Eng.* **40,** 61–68.

TAYLOR, G. I. 1961 Deposition of a viscous fluid on the wall of a tube. *J. Fluid Mech.* **10,** 161–165.

ZUKOSKI, E. E. 1966 Influence of viscosity, surface tension, and inclination angle on motion of long bubbles in closed tubes. *J. Fluid Mech.* **25,** 821–837.

APPENDIX: COEFFICIENTS OF THE POWER SERIES EXPANSION

Consider the following power series expansions of the Bessel and exponential functions to the sixth order in ξ and fourth order in η:

$$J_0(\beta_i\xi) = 1 - \frac{1}{1}\left(\frac{\beta_i}{2}\right)^2\xi^2 + \frac{1}{(2!)^2}\left(\frac{\beta_i}{2}\right)^4\xi^4 - \frac{1}{(3!)^2}\left(\frac{\beta_i}{2}\right)^6\xi^6 + O(\xi^8)\cdots$$

$$J_1(\beta_i\xi) = \left(\frac{\beta_i}{2}\right)\xi - \frac{1}{1!2!}\left(\frac{\beta_i}{2}\right)^3\xi^3 + \frac{1}{2!3!}\left(\frac{\beta_i}{2}\right)^5\xi^5 - O(\xi^7) \qquad [A1]$$

$$e^{-\beta_i\eta} = 1 - 2\left(\frac{\beta_i}{2}\right)\eta + \frac{2^2}{2!}\left(\frac{\beta_i}{2}\right)^2\eta^2 - \frac{2^3}{3!}\left(\frac{\beta_i}{2}\right)^3\eta^3 + \frac{2^4}{4!}\left(\frac{\beta_i}{2}\right)^4\eta^4 + O(\eta^5)\cdots$$

Define the constants B_m by

$$B_m = \sum_{i=1}^{N} k_i\left(\frac{\beta_i}{2}\right)^m, \quad m = 2, \ldots, N+1. \qquad [A2]$$

The bubble surface equation [19] is then to the order $O(\xi^6)$ and $O(\eta^3)$ for $\xi \neq 0$:

$$\xi \cdot \left\{ -\tfrac{1}{2} \sum_i k_i \beta_i - \frac{v_m}{4} \xi^2 + \frac{1}{\xi} \sum_i k_i J_1(\beta_i \xi) \, e^{-\beta_i \eta} \right\} = 0.$$

Applying the expansions [A1] yields

$$\left[-\left(\frac{B_3}{1!2!} + \frac{v_m}{4} \right) \xi^2 + \frac{B_5}{2!3!} \xi^4 - \frac{B_7}{3!4!} \xi^6 + \cdots \right] - \frac{2}{1!} \left(B_2 - \frac{B_4}{1!2!} \xi^2 + \frac{B_6}{2!3!} \xi^4 \right) \eta$$
$$- \frac{2^2}{2!} \left(B_3 - \frac{B_5}{1!2!} \xi^2 + \frac{B_7}{2!3!} \xi^4 \right) \eta^2 - \frac{2^3}{3!} \left(B_4 - \frac{B_6}{1!2!} \xi^2 \right) \eta^3 = 0.$$

From Dumitrescu (1943), Davies and Taylor (1949) and others, we know that for small Σ, at least, the bubble shape is nearly spherical at its nose, and η is at least of order 2 in ξ. Thus to $O(\xi^6)$ we have

$$-\tfrac{8}{6} B_4 \eta^3 + [2B_3 - B_5 \xi^2] \eta^2 - 2 \left(B_2 - \frac{B_4}{2} \xi^2 + \frac{B_6}{12} \xi^4 \right) \eta$$
$$- \frac{1}{2} \left(B_3 + \frac{v_m}{2} \right) \xi^2 + \frac{B_5}{12} \xi^4 - \frac{B_7}{144} \xi^6 = 0. \qquad \text{[A3]}$$

A natural next step would be to represent η by a power series function of ξ^2, possibly spherical near origo, as assumed by Dumitrescu (1943). With surface tension effects present, however, the bubble shape near origo will be quite deformed, and the above approximation becomes too crude. Instead we solve for η from [A3], considering it a second order equation in η

$$\eta = \left(2 \left(B_2 - \frac{B_4}{2} \xi^2 + \frac{B_6}{12} \xi^4 \right) \pm 2 \left\{ \left(B_2 - \frac{B_4}{2} \xi^2 + \frac{B_6}{12} \xi^4 \right)^2 + (2B_3 - B_5 \xi^2) \right. \right.$$
$$\left. \left. \cdot \left[\frac{1}{2} \left(B_3 + \frac{v_m}{2} \right) \xi^2 - \frac{B_5}{12} \xi^4 + \frac{B_7}{144} \xi^6 - \tfrac{8}{6} B_4 \eta^3 \right] \right\}^{1/2} \right) \cdot [2(2B_3 - B_5 \xi^2)]^{-1}.$$

With the actual choice of coordinate system, the bubble surface is completely below origo, and the negative sign must be retained. Expanding the square root in powers of ξ^2 we get to $O(\xi^6)$:

$$\eta = \left\{ \left(B_2 - \frac{B_4}{2} \xi^2 + \frac{B_6}{12} \xi^4 \right) - B_2 \right.$$
$$\left. - B_2 \left[\frac{a}{2} \xi^2 - \frac{1}{2} \left(b - \tfrac{1}{4} a^2 \right) \xi^4 + \frac{1}{6} \left(3c - \tfrac{3}{2} ab + \frac{3a^3}{8} \right) \xi^6 \right] \right\} \Big/ (2B_3 - B_5 \xi^2), \qquad \text{[A4]}$$

where

$$a = (B_3^2 + \tfrac{1}{2} B_3 v_m - B_2 B_4) B_2^{-2},$$
$$b = (\tfrac{1}{4} B_4^2 - \tfrac{2}{3} B_3 B_5 - \tfrac{1}{4} B_5 v_m + \tfrac{1}{6} B_2 B_6) B_2^{-2}, \qquad \text{[A5]}$$
$$c = \tfrac{1}{12} (B_5^2 - B_4 B_6 + \tfrac{1}{6} B_3 B_7 + \tfrac{8}{3} B_4 \eta^3) B_2^{-2}.$$

Rearranging [A4] in increasing order of ξ we finally get

$$\eta = (-a_1 \xi^2 - a_2 \xi^4 - a_3 \xi^6) \cdot [2(2B_3 - B_5 \xi^2)]^{-1}, \qquad \text{[A6]}$$

where $B_{3v} = B_3 + v_m/2$,

$$\begin{aligned} a_1 &= (B_3/B_2)B_{3v}, \\ a_2 &= B_2[b - \tfrac{1}{4}a^2 - \tfrac{1}{6}(B_6/B_2)], \\ a_3 &= \tfrac{1}{3}B_2(3c - \tfrac{3}{2}ab + \tfrac{3}{8}a^3). \end{aligned} \qquad [A7]$$

Equation [A6] is an explicit one for η; i.e., if the coefficients B_m are known, the bubble shape near origo may be obtained. With $N = 3$ in [19] and [20] three of the coefficients B_m, $m = 2, 4$ may be obtained from [20] as follows.

Firstly, the expansion [A1] is substituted in [20], yielding to $O(\xi^6)$

$$\begin{aligned} &[4(B_2^2\xi^2 - B_2B_4\xi^4 + \tfrac{1}{4}B_4^2\xi^6) + \tfrac{2}{3}B_2B_6\xi^6 - 16B_2B_3\xi^2\eta + 8(B_3B_4 + B_2B_5)\xi^4\eta \\ &\quad + 16B_2B_4\xi^2\eta^2 + 16B_3^2\xi^2\eta^2] + \{4(B_{3v}^2\xi^4 - \tfrac{1}{2}B_5B_{3v}\xi^6) \\ &\quad - 16(-B_{3v}\xi^2 + \tfrac{1}{4}B_5\xi^4) \cdot [(B_2 - B_4\xi^2)\eta - B_3\eta^2] \\ &\quad + 16(B_2^2 - 2B_2B_4\xi^2)\eta^2\} = 2\,|\,\eta\,| - 2 \cdot \Sigma[2/R_0 - 2/R(\eta)]. \end{aligned} \qquad [A8]$$

Rearranging this equation, we get

$$\begin{aligned} &B_2^2\xi^2 + (B_{3v}^2 - B_2B_4)\xi^4 + (\tfrac{1}{4}B_4^2 + \tfrac{1}{6}B_2B_6 - \tfrac{1}{2}B_{3v}B_5)\xi^6 \\ &\quad + [2B_2v_m\xi^2 - (2B_3B_4 + 2B_4v_m - B_2B_5)\xi^4]\eta + [-(2B_3v_m + 4B_2B_4)\xi^2 + 4B_2^2]\eta^2 \\ &\qquad = \tfrac{1}{2}\,|\,\eta\,| - \tfrac{1}{2}\Sigma[1/R_0 - 1/R(\eta)]. \end{aligned} \qquad [A9]$$

To proceed expressions for the radii of curvature are needed. Approximating the surface equation, [A3] with a power series in ξ^2, $\eta = -\Sigma_{i=1}^{N}\,|\,b_i\,|\,\xi^{2i}$ in [21], differentiating with respect to ξ, yields

$$\frac{\partial\eta}{\partial\xi} = -\sum_{i=1}^{N+1} 2ib_i\xi^{2i-1}$$

and [A10]

$$\frac{\partial^2\eta}{\partial\xi^2} = \sum_{i=1}^{N+1} 2i(2i-1)b_i\xi^{2(i-1)},$$

where

$$\begin{aligned} b_1 &= a_1/4B_3, \\ b_2 &= (-2B_3b_1^2 + B_4b_1 - \tfrac{1}{12}B_5)/2B_2, \\ b_3 &= (-4B_3b_1b_2 + B_5b_1^2 + B_4b_2 - \tfrac{1}{6}B_6b_2 + \tfrac{1}{144}B_7 - \tfrac{4}{3}B_4a_1^3)/2B_2, \\ b_4 &= [-2B_3(b_2^2 + 2b_1b_3) + 2B_5b_1b_2 + B_4b_3 - \tfrac{1}{6}B_6b_2 - 4B_4b_1^2b_2, \\ &\quad - (1/4!5! - 2/3!4!)B_8 - \tfrac{1}{6}B_7b_1^2 + \tfrac{2}{3}B_6b_1^3]/2B_2. \end{aligned}$$

Thus

$$2/R_0 = 2b_1 + 2b_1 = 4b_1.$$

Obviously, including all surface tension terms of order six, requires the bubble surface equation [A6] to be of order $O(\xi^8)$, and this was done in order to obtain b_4. Then, from [21] after some algebra, we get

$$\frac{1}{R_1(\eta)} = 2b_1 + 12(b_2 - b_1^3)\xi^2 + 30(b_3 - 4b_1^2b_2 + 2b_1^5)\xi^4 + 28(b_4 - 12b_1b_2^2 - 9b_1^2b_3 + 30b_1^4b_2 - 10b_1^7)\xi^6 \quad [A11]$$

and

$$\frac{1}{R_2(\eta)} = 2b_1 + 4(b_2 - b_1^3)\xi^2 + 6(b_3 - 4b_1^2b_2 + 2b_1^5)\xi^4 + 4(b_4 - 12b_1b_2^2 - 9b_1^2b_3 + 30b_1^4b_2 - 10b_1^7)\xi^6.$$

It is now easily ascertained that for a spherical bubble surface the expressions in the brackets are zero to $O(\xi^6)$; thus the curvatures are constant and equal for all ξ, as they should.

From [A11] the surface tension term in [A9] becomes

$$-\frac{1}{2}\Sigma\left[\frac{1}{R_0} - \frac{1}{R(\eta)}\right] = \frac{1}{2}\Sigma\,[16\,(b_2 - b_1^3)\,\xi^2 + 36(b_3 - 4b_1^2b_2 + 2b_1^5)\xi^4 + 32(b_4 - 12b_1b_2^2 - 9b_1^2b_3 + 30b_1^4b_2 - 10b_1^7)\xi^6] \quad [A12]$$

Inserting [A6] for η and [A12] in [A9] finally yields

$$\begin{aligned}
&\left[4B_3B_2^2 - \frac{1}{2}a_1 - 8\Sigma(b_2 - b_1^3)4B_3\right]\xi^2 + \left\{5B_3B_{3v}^2 - 4B_2B_3B_4 - 2B_2^2B_5 - 2B_3B_{3v}v_m\right.\\
&\quad - \frac{1}{2}a_2 - \Sigma\cdot\left[18(b_3 - 4b_1^2b_2 + 2b_1^5)4B_3 - 16B_5(b_2 - b_1^3)\right]\Bigg\}\xi^4\\
&\quad + \left(\left[\frac{B_3}{B_2}B_{3v}^2 + 2B_{3v}B_3(B_3 + v_m) + 2B_2B_5\right]B_4 + B_3\cdot B_4^2\right. \qquad [A13]\\
&\quad + \left\{\left[-\frac{3}{2}B_5 - \frac{v_m}{2}\frac{B_3^2}{B_2^2}\right]B_{3v} - 3B_3B_5\right\}B_{3v} + \frac{2}{3}B_2B_3B_6 + 2B_2(1 - v_m)a_2 - \frac{1}{2}a_3\\
&\quad - \sum\,[64B_3(b_4 - 12b_1b_2^2 - 9b_1^2b_3 + 30b_1^4b_2 - 10b_1^7)\\
&\quad \left. - 36B_5\cdot(b_3 - 4b_1^2b_2 + 2b_1^5)]\right)\xi^6 = 0.
\end{aligned}$$